THE JOURNAL OF BIOLOGICAL CHEMISTRY
Vol. 276, No. 23, Issue of June 8, pp. 20491–20498, 2001

Printed in U.S.A.

Vacuolar Localization of Oligomeric α-Mannosidase Requires the Cytoplasm to Vacuole Targeting and Autophagy Pathway Components in *Saccharomyces cerevisiae**

Received for publication, February 6, 2001, and in revised form, March 15, 2001
Published, JBC Papers in Press, March 22, 2001, DOI 10.1074/jbc.M101150200

Maria U. Hutchins and Daniel J. Klionsky‡

From the Department of Biology, University of Michigan, Ann Arbor, Michigan 48109

One challenge facing eukaryotic cells is the post-translational import of proteins into organelles. This problem is exacerbated when the proteins assemble into large complexes. Aminopeptidase I (API) is a resident hydrolase of the vacuole/lysosome in the yeast *Saccharomyces cerevisiae*. The precursor form of API assembles into a dodecamer in the cytosol and maintains this oligomeric form during the import process. Vacuolar delivery of the precursor form of API requires a vesicular mechanism termed the cytoplasm to vacuole targeting (Cvt) pathway. Many components of the Cvt pathway are also used in the degradative autophagy pathway. α-Mannosidase (Ams1) is another resident hydrolase that enters the vacuole independent of the secretory pathway; however, its mechanism of vacuolar delivery has not been established. We show vacuolar localization of Ams1 is blocked in mutants that are defective in the Cvt and autophagy pathways. We have found that Ams1 forms an oligomer in the cytoplasm. The oligomeric form of Ams1 is also detected in subvacuolar vesicles in strains that are blocked in vesicle breakdown, indicating that it retains its oligomeric form during the import process. These results identify Ams1 as a second biosynthetic cargo protein of the Cvt and autophagy pathways.

One of the hallmarks of eukaryotic cells is the presence of a variety of membrane enclosed organelles. These compartments are critical to the proper physiology of the cell. In order to ensure correct function, cells must maintain faithful sorting of resident proteins to each organelle. A substantial amount of information is known about the delivery of proteins to compartments of the endomembrane system including the endoplasmic reticulum (ER),[1] Golgi complex, and vacuole/lysosome. In brief, proteins can enter the ER post-translationally through proteinaceous channels and transit to other compartments through transient carrier vesicles. However, other compartments are not able to receive proteins through this route. For example, peroxisomes, mitochondria, and chloroplasts maintain a separate mechanism(s) for translocating proteins across their membranes (1–3).

One challenge facing eukaryotic cells is the import of large assembled protein complexes into organelles. Although several organelles have the capacity to translocate folded proteins (4), in most cases complexes assemble subsequent to import of the individual protein monomers. In contrast, the peroxisome has the capacity for importing oligomeric proteins directly from the cytosol (5). Several components in peroxisome protein import are currently being characterized, but the actual mechanics of import are not defined (3). Both a transient pore/shuttle or a vesicular invagination of the peroxisome membrane could act in conjunction with the known receptor proteins. Although most vacuolar proteins enter the vacuole through a portion of the secretory pathway, the resident hydrolase aminopeptidase I (API) uses an alternative process (6). Precursor API (prAPI) is synthesized in the cytosol on ribosomes that are not attached to the ER. Following synthesis, prAPI rapidly assembles into a dodecamer and subsequently into a higher order complex (7). This complex of dodecamers becomes sequestered by membrane, resulting in the formation of a double-membrane cytosolic vesicle (8, 9). Upon completion, this vesicle fuses with the vacuole to release a single-membrane vesicle into the lumen. Following breakdown of the vesicle, prAPI is matured by removal of its propeptide. This import process is termed the cytoplasm to vacuole targeting (Cvt) pathway. The Cvt pathway has been shown to overlap with autophagy (10, 11). Autophagy is a degradative process that employs similar changes in membrane topology to sequester cytosol for breakdown and recycling under starvation conditions. During starvation, the level of prAPI increases and the protein is imported to the vacuole via autophagosomes (9). An intriguing question has been why yeast cells have utilized such a complex process as the Cvt pathway for the import of a resident vacuolar hydrolase. One possibility is that the dodecameric structure of prAPI is critical for its stability and/or function. The size of the dodecamer prevents translocation through the ER translocon, necessitating a vesicle-mediated import process. In addition, it has not been known whether other resident hydrolases utilize the Cvt pathway for vacuolar localization.

α-Mannosidase (Ams1) is a resident vacuolar hydrolase that has been shown to enter the vacuole independent of the secretory pathway (12). As a resident vacuolar hydrolase, one role of

* This work was supported by Public Health Service Grant GM53396 from the National Institutes of Health (to D. J. K.) and National Science Foundation Plant Cell Biology Training Grant DIR 90-14274 (to M. U. H.). The costs of publication of this article were defrayed in part by the payment of page charges. This article must therefore be hereby marked "*advertisement*" in accordance with 18 U.S.C. Section 1734 solely to indicate this fact.

‡ To whom correspondence should be addressed: Dept. of Biology, University of Michigan, 830 N. University Ave., Ann Arbor, MI 48109. Tel.: 734-615-6556; Fax: 734-647-0884; E-mail: klionsky@umich.edu.

[1] The abbreviations used are: ER, endoplasmic reticulum; Ams1, vacuolar α-mannosidase; Apg, autophagy; API, aminopeptidase I; CPY, carboxypeptidase Y; Cvt, cytoplasm to vacuole targeting; FM 4–64, *N*-(3-triethylammoniumpropyl)-4-(6-(4-(diethylamino)phenyl)hexatrienyl)pyridinium dibromide; HA, hemagglutinin epitope; prAPI, precursor aminopeptidase I; SD−N, synthetic minimal medium lacking nitrogen; SGd, synthetic minimal medium containing 3% glycerol; SMD, synthetic minimal medium containing nitrogen; YFP, yellow fluorescent protein; YNB, yeast nitrogen base; βOG, *n*-octyl-β-D-glucopyranoside; MES, 2-(*N*-morpholino)ethanesulfonic acid; MOPS, 3-(*N*-morpholino)propanesulfonic acid; kb, kilobase pair(s); PAGE, polyacrylamide gel electrophoresis; TSB, Tris salts buffer.

Ams1 is to aid in recycling macromolecular components of the cell through hydrolysis of terminal, non-reducing α-D-mannose residues (EC 3.2.1.24). In growing wild type cells, a relatively low basal level of Ams1 is synthesized. Under conditions of greater recycling need (*i.e.* nutrient deprivation), Ams1 levels are induced, and this coincides with induction of the nonspecific delivery mechanism of autophagy. We show in this report that Ams1 forms an oligomer in the cytoplasm. Under nutrient-rich conditions, oligomeric Ams1 is delivered to the vacuole by the Cvt pathway. Under starvation conditions, the up-regulated oligomeric protein is localized through autophagy. Mutants in either pathway are defective in Ams1 import. These results define Ams1 as a second cargo protein that utilizes both the Cvt and autophagic pathways for biosynthetic delivery to the vacuole.

EXPERIMENTAL PROCEDURES

Reagents—Prestained molecular weight markers were from Bio-Rad. Oligonucleotide primers were synthesized by Operon Technologies (Alameda, CA). The pAM1 plasmid (13) was a gift from Drs. Michael J. Kuranda and Phillips W. Robbins (Massachusetts Institute of Technology, Cambridge, MA). Yeast nitrogen base (YNB) was from Difco. YNB without copper ions was from BIO 101 (Vista, CA). Ficoll, DEAE-dextran, and the Vistra ECF Western blotting reagents were from Amersham Pharmacia Biotech. Restriction enzymes, ligase, and DNA polymerase were from New England Biolabs (Beverly, MA). Yeast lytic enzyme was from ICN Biomedicals (Aurora, OH). Complete EDTA-free protease inhibitors were from Roche Molecular Biochemicals. *n*-Octyl-β-D-glucopyranoside detergent (βOG) was from Calbiochem (La Jolla, CA). *N*-(3-triethylammoniumpropyl)-4-(6-(4-(diethylamino)phenyl) hexatrienyl)pyridinium dibromide (FM 4–64) was from Molecular Probes (Eugene, OR). Polyclonal antiserum to the HA epitope was from Santa Cruz Biotechnology (Santa Cruz, CA). Other reagents were from Sigma unless noted.

Strains and Growth Conditions—Strains used were SEY6210 *MATα ura3–52 leu2–3,112 his3-Δ200 trp1-Δ901 lys2–801 suc2-Δ9 mel GAL* (14); JKY007, SEY6210 *agp9*Δ (15); AHY1468, SEY6210 *apg1*/*cvt10–4*; THY193, SEY6210 *apg7*/*cvt2–1*; AHY1293, SEY6210 *apg14*/*cvt12–1*; THY313, SEY6210 *aut7*/*cvt5–1*; THY119, SEY6210 *cvt3–1*; AHY96, SEY6210 *cvt9–1*; THY32, SEY6210 *cvt17–1* (10, 16). MHY10 (SEY6210 *pep4*Δ::*URA3*) was generated as described for MHY8 (17). THY411 (SEY6210 *ams1*Δ::*LEU2*) was generated by transforming yeast with *Pvu*II-linearized pDelLAMS (described below), which replaces the first third of the chromosomal *AMS1* gene with *LEU2*. The 3×HA-tagged Ams1 strain MHY11 was generated by the integration of a DNA fragment encoding the 3×HA epitope at the 3′ end of the chromosomal *AMS1* locus in strain SEY6210 using the ME3 plasmid (provided by Dr. Neta Dean, State University of New York, Stony Brook, NY) as a template (primers: AMSPREHA (5′-AATTGAGACCTTTTGAGATTGC-CTCATTCAGGTTGTATTTCTACCCATACGATGTTCCT-3′) and AMSpastHA (5′-TTTACTTATATGTATTTTGTTAAGACTATTTTTGG-TTATCAGTCGACGGTATCGATAAG-3′)). Confirmation of the integrated *AMS1*::*AMS1*-HA was shown by induction of a ~132-kDa fusion protein. Integration of the HA epitope at the chromosomal *AMS1* locus had no detectable effect on Ams1 activity or its vacuolar localization (data not shown).

Strains were typically grown on SMD (0.67% YNB, 2% glucose). Strains were also grown to a density of 0.5 A_{600} in SMD and were resuspended and grown in SGd (0.67% YNB, 3% glycerol, 0.1% glucose) for induction of Ams1 where indicated. Strains that were induced with 10 or 50 μM copper sulfate were first subcultured three times in SMD lacking copper ions. All media were brought to pH 5.5 with 50 mM each MES and MOPS and supplemented with required amino acids and vitamins.

Plasmids—The copper-inducible *AMS1* plasmids pCuAMS1(414) and pCuAMS1(424) (pMUH25 and pMUH26, respectively) were generated as follows. Oligonucleotide primers (AM1LOWSPE, 5′-CAAAAAC-TAGTAATTATGTCATC-3′; and AM1UP2, 5′-CGCTTGCTCGAGCTC-CTCTATGTGGATAG-3′) were used to amplify a truncated *AMS1* sequence from pAM1 (13). The 2.9-kb product was ligated into pCR-Blunt (Invitrogen, Carlsbad, CA), resulting in a 6.4-kb construct with flanking *Spe*I sites (pMUH18). pMUH18 was digested with *Spe*I, and the resulting 2.9-kb fragment was ligated in the correct orientation at the *Spe*I site of plasmid pCu414 (provided by Dr. Dennis J. Thiele, University of Michigan, Ann Arbor, MI; Ref. 18), resulting in a 7.8-kb plasmid (pMUH21). To restore the full-length sequence of *AMS1*, the *AMS1* gene was amplified from the pAM1 plasmid (primers: AM1LOWER, 5′-CCTAACTCGTTTAAGGGAGAC-3′; and AM1UPPER, 5′-CAGTGAGGGAGACAAACTCAG-3′). A 3.4-kb product was ligated into pCR-Blunt to generate a 6.9-kb plasmid (pMUH10). The 3.5-kb *Xho*I/*Spe*I fragment from pMUH10 was ligated into the same sites of pRS423 (19) generating pMUH12. The carboxyl terminus of *AMS1* was restored with the 525-base pair *Sph*I/*Xho*I fragment from pMUH12 ligated into pMUH21 resulting in the centromeric (CEN) plasmid pCuAMS1(414) (pMUH25). The multicopy (2μ) plasmid pCuAMS1(424) (pMUH26) was generated by ligating the 2.9-kb *Spe*I fragment from pMUH18 into the *Spe*I site of pCu424 (18), resulting in an 8.5-kb plasmid (pMUH22). The carboxyl terminus of *AMS1* was restored as described for pMUH25.

pCuAMS1YFP (pMUH29) was generated from pMUH21 and the 780-base pair fragment from pEYFP (CLONTECH, Palo Alto, CA), each digested with *Sph*I/*Eco*RI. The resulting fusion protein contained the amino-terminal 929 amino acid residues from Ams1 followed by a 14-amino acid linker and YFP sequence.

The *ams1*Δ*::LEU2* deletion plasmid, pDelLAMS1, was generated from a 1-kb upstream portion and a 1.5-kb interior portion of the *AMS1* gene isolated separately from pAM1 by a *Xho*I/*Hin*dIII digest and a *Bgl*II/*Eco*RI/*Hin*dIII digest, respectively. These fragments were ligated in the vector pRS306 (19) resulting in a unique *Hin*dIII site between the two segments of *AMS1*. This plasmid was digested with *Hin*dIII, and a *Hin*dIII fragment containing the *LEU2* gene was cloned into this site to generate plasmid pDelLAMS1.

The plasmid pCYI-50 (20) encodes the first 50 amino acids of carboxypeptidase Y (CPY) including the vacuolar targeting signal, fused to the periplasmic protein invertase, lacking its amino-terminal signal sequence in the vector pSEYC306. The plasmid pLJL2 is similar to pCYI-50 but carries the *LEU2* gene instead of *URA3*.

Vacuole Preparations—Vacuoles were isolated on a Ficoll step gradient essentially as described previously (21) with minor adaptations. Cells were grown in SMD to early log phase, and then ~500 A_{600} units were harvested and spheroplasted with 6–10 mg of yeast lytic enzyme. Ninety percent or greater spheroplasting efficiency was determined by comparing the A_{600} of cells diluted 1:10 in water before and after addition of lytic enzyme. The plasma membrane was lysed using 400 μl of a 0.4 mg/ml solution of DEAE-dextran by being chilled on ice for 2 min, shaken at 30 °C for 2.5 min, and placed on ice again. 3 ml of lysed cell solution containing 2 mM phenylmethylsulfonyl fluoride were loaded at the bottom of an ultraclear SW41 tube (Beckman Coulter, Fullerton, CA) and overlaid with 8%, 4%, and 0% Ficoll solutions. Vacuoles were collected from the 0%/4% float interface with a Pasteur pipette after a 1.5-h spin at 30,000 × *g*. Enzyme assays for marker proteins were performed on material loaded onto the gradient and the recovered vacuole float fraction.

Enzyme Assays—Cell lysates and harvested vacuoles were assayed for marker enzymes invertase, α-glucosidase, and NADPH-cytochrome *c* reductase as described (20). Ams1 activity was determined based on established protocol (22). Samples were treated with Triton X-100 (2.5% final concentration), and then the volume was brought up to 400 μl with distilled H_2O. 100 μl of 5× substrate mix (200 mM sodium acetate, pH 6.5, 2 mM *p*-nitrophenyl-α-D-mannopyranoside) was added to start the reaction and was incubated for 1 h at 37 °C. The reaction was stopped with 200 μl of 10% trichloroacetic acid, and any particulates were spun down in a microcentrifuge for 5 min. An equal volume of 1 M glycine, pH 10.4, was added to neutralize the reaction before the absorbance at 400 nm was read. Results from assays for each strain were tabulated from a minimum of four independent vacuole preparations.

Immunoblotting and Antisera—Antisera was generated to Ams1 using two synthetic peptides (Multiple Peptide Systems, San Diego, CA) corresponding to amino acid residues 79–96 and residues 991–1011. These peptides were conjugated to keyhole limpet hemocyanin and injected into a New Zealand White male rabbit using standard procedures. Immunoblots were prepared from 8% SDS-PAGE gels as described (16) with 15% methanol in the transfer buffer. Ams1 antiserum was blocked by incubating with *ams1*Δ cell extract in TTBS (20 mM Tris, pH 7.6, 0.8% NaCl, 0.1% (w/v) Tween 20) for 2–3 h at 4 °C prior to use at a 1:12,500 dilution for 4 h at room temperature. Polyclonal antiserum to the HA epitope was used at a 1:1,000 dilution. API antiserum was described previously (6). Quantitation by Vistra kit or use of secondary antibodies conjugated to horseradish peroxidase was as described (16, 17). Immunoblots were quantified on a STORM PhosphorImager (Molecular Dynamics, Sunnyvale, CA).

Glycerol Gradient—Strains harboring the pCuAMS1(414) plasmid encoding *AMS1* under a copper regulable promoter were grown in SMD

in the absence of copper. The presence of this plasmid facilitated the visualization of Ams1 under the indicated growth conditions. Cells were induced with 50 μM $CuSO_4$ for 1 h. Twenty A_{600} units were harvested in log phase and washed in Tris salts buffer (TSB; 50 mM Tris, pH 8.5, 50 mM KOAc, 100 mM KCl, 0.5 mM $MgCl_2$). Cells were transferred to a microcentrifuge tube and resuspended in 250 μl of TSB containing 1 μg/ml pepstatin A and Complete EDTA-free protease inhibitors. Cells were lysed with glass beads for 1 min, and then βOG was added to 2% final concentration and mixed gently with a pipette tip. 200 μl of sample was loaded on a 1.8-ml prepoured 20–50% glycerol gradient made up in TSB and containing protease inhibitors. Oligomeric complexes were resolved at 55,000 rpm for 4 h in a Beckman TLS-55 rotor at 15 °C.

Ten supernatant fractions of 200 μl were collected from the top of the gradient and precipitated with 10% trichloroacetic acid on ice. Fraction 10 may contain some amount of contaminating pellet material. Samples were washed twice in acetone and sonicated in MES/urea resuspension buffer (6) before resolving by SDS-PAGE, followed by immunoblot and detection of Ams1 or API. A higher molecular mass cross-reactive protein detected by Ams1 antiserum (see Fig. 1*B*, *lane 5*) migrated to fractions 3–4 in wild type and *cvt2* cells (Fig. 3, *A* and *B*). Quantification of these fractions was arbitrarily set to zero for clarity. Protein standards were run on an identical gradient and the peak fraction for each was determined by Coomassie Brilliant Blue staining of a SDS-PAGE gel. Bovine serum albumin (66 kDa), aldolase (158 kDa), and catalase (240 kDa), peaked in fractions 3, 4, and 5, respectively, whereas apoferritin (450 kDa), urease (545 kDa) and thyroglobulin (669 kDa) all peaked in fraction 6 of the gradient.

For separation of the MHY11 vacuole fraction on a glycerol gradient, purified vacuoles were collected as described above and 10× TSB was added to 1× prior to a 5-min, 4 °C centrifugation step at 13,000 rpm. The pellet containing the concentrated vacuoles was resuspended in 250 μl of TSB plus inhibitors and detergent and mixed, and 200 μl was loaded onto the gradient and collected as above.

Fluorescence Microscopy—Confocal microscopy (Leica IRM confocal microscope) images were taken as an average of 4–8 scans of a single focal plane. Cells harboring the pCuAMS1YFP plasmid (pMUH29) were grown to early log phase and induced with 10 μM copper sulfate for 12 h. 1 ml of cells were then harvested and resuspended with 100 μl of fresh medium containing 4–8 μM FM 4–64 (23) for 30 min to label the vacuoles. FM 4–64 was chased to the vacuole for 1 h by the addition of 1 ml of fresh medium. Cells were then washed once in SD−N (containing 10 μM copper sulfate) and incubated in fresh SD−N for 12 h.

RESULTS

Ams1 Delivery to the Vacuole under Vegetative Conditions Is Dependent on Machinery of the Cvt and Autophagy Pathways—Most of the characterized vacuolar hydrolases are proteolytically processed upon delivery to the vacuole. The resulting shift in molecular mass provides a convenient means for monitoring delivery to the organelle. We were interested in determining the mechanism of vacuolar delivery used by the resident hydrolase α-mannosidase (Ams1). However, previous analyses of Ams1 have been equivocal with regard to whether this protein is rapidly processed following delivery to the vacuole (12, 24). To examine processing of Ams1, we generated antiserum to synthetic peptides corresponding to the deduced amino acid sequence as described under "Experimental Procedures." We were unable to detect Ams1 synthesized from the chromosomal locus when cells were grown in minimal medium (SMD). This result was not surprising because Ams1 is made at very low levels in the presence of glucose unless cells are subjected to heat shock (12, 22, 24). However, when Ams1 was synthesized from a CEN or 2μ plasmid, we were able to detect a specific band in a dosage-dependent manner (Fig. 1*A*).

Ams1 has a predicted molecular mass of 124 kDa. Previous studies indicated that the initial protein product was 107 kDa and that this was processed to 73 and 31 kDa forms that co-purified (24). However, we detected a band corresponding to Ams1 that migrated at 122 kDa (Fig. 1*B*) that is closer in agreement with the expected molecular mass and probably corresponds with the full-length protein. To increase the level of Ams1, we expressed the protein from a CEN plasmid under control of the *CUP1* promoter. A 73-kDa cleavage product was

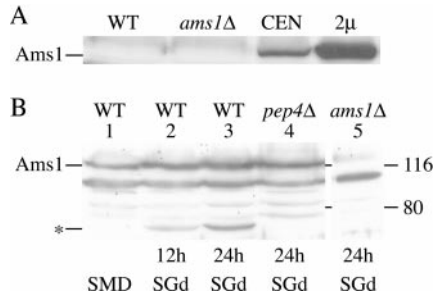

FIG. 1. **Biosynthesis of Ams1.** *A*, antiserum to Ams1 recognizes a 122-kDa band. Wild type (SEY6210; *lane 1*), *ams1*Δ (*lane 2*), and wild type cells harboring *AMS1* on a CEN or 2μ plasmid (*lanes 3* and *4*) were grown in SMD to the early log phase. Ams1 expressed from plasmids is detected in a dosage-dependent manner. Plasmid-containing strains were induced with 50 μM copper sulfate for 40 min prior to harvest. Cells were lysed with glass beads and run on an 8% SDS-PAGE gel for immunoblot detection using anti-Ams1 antiserum. 1.0 A_{600} equivalent units of extract was loaded in *lanes 1* and *2* and 0.25 units in *lanes 3* and *4*. *B*, Pep4-dependent Ams1 cleavage is not a direct indication of vacuolar delivery. Steady-state levels of Ams1 are shown at various conditions for several strains. Strains in *lanes 1–4* contain the CEN *AMS1* plasmid pCuAMS1(414). *Lane 1*, wild type cells grown to early log phase in SMD and induced for 40 min with 50 μM copper sulfate. *Lanes 2* and *3*, wild type cells shifted 12 or 24 h to SGd (containing 10 μM copper sulfate), respectively. The level of Ams1 is increased, and a 73-kDa cleavage product (indicated by the *asterisk*) appears as cells are deprived of glucose (*lanes 2* and *3*). *Lane 4*, *pep4*Δ cells shifted 24 h to SGd (containing 10 μM copper sulfate). Lack of the 73-kDa species indicates this cleavage event is Pep4-dependent. *Lane 5*, *ams1*Δ cells shifted 24 h to SGd (containing 10 μM copper sulfate) is shown as a control for cross-reactive protein recognized by the anti-Ams1 antiserum. *WT*, wild type.

not detected in wild type cells grown in SMD (Fig. 1*B*, *lane 1*). After cells were grown to early log phase and shifted to glycerol medium (SGd), a 73-kDa protein was apparent that first appeared ~12 h after the shift. This band increased in abundance from 12 to 24 h (Fig. 1*B*, *lanes 2* and *3*). Appearance of the 73-kDa species was not seen in a *pep4*Δ strain (Fig. 1*B*, *lane 4*), indicating that it was due to a vacuole-dependent cleavage event in agreement with previous studies (12). However, the slow kinetics of cleavage and the observation that processing was incomplete, coupled with the fact that this processing event is not required for Ams1 enzymatic activity (12), suggest that the cleavage event may be a byproduct of vacuolar localization. Accordingly, processing of Ams1 is not a good indicator for a kinetic analysis of vacuolar delivery.

Because Ams1 is not processed concomitant with its delivery to the vacuole, we could not rely on a mobility shift to follow localization. As an alternative approach, we analyzed its localization through subcellular fractionation. Yeast cells were grown to early log phase in minimal medium, and vacuoles were isolated on a Ficoll step gradient as described under "Experimental Procedures." The efficiency of vacuolar recovery was determined by assessing the invertase activity of a vacuolar targeted fusion protein consisting of a portion of the resident vacuolar protease CPY fused to the marker protein invertase (20). This chimeric construct utilizes the vacuolar targeting signal in CPY to divert the periplasmic enzyme invertase from the secretory pathway to the vacuole. The percentage of invertase activity in the purified vacuole fraction relative to the activity in a total spheroplast lysate provides a measure for the efficiency of organelle purification. Vacuole recovery of the CPY-invertase hybrid protein typically was 20% or higher as compared with the activity in the total fraction. In wild type cells, Ams1 activity in the purified vacuolar fraction was essentially equivalent to the vacuolar recovery based on invertase activity from the CPY-invertase marker (Fig. 2*A*). This result indicates that vacuole purification is an effective method

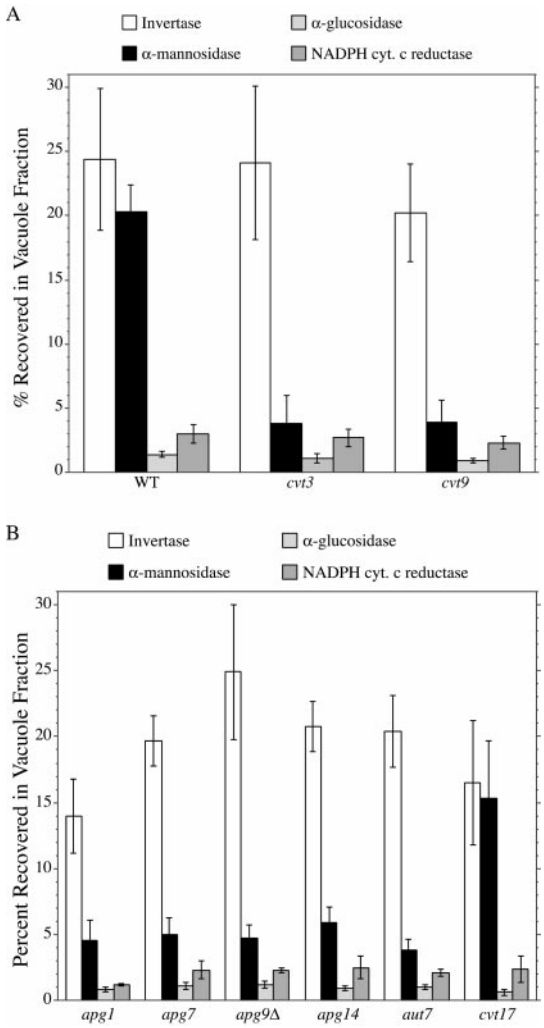

FIG. 2. **Vacuole delivery of Ams1 is defective in *cvt*, *apg*, and *aut* mutants.** *A*, mutants specific to the Cvt pathway do not import Ams1 into the vacuole. Vacuoles were isolated on Ficoll step gradients as described under "Experimental Procedures." Activity assays of Ams1 and marker proteins show equivalent recovery of Ams1 and CPY-invertase in the vacuole fraction of wild type (*WT*) cells, but not in the vacuole fraction purified from the *cvt3* and *cvt9* mutant strains. CPY-invertase (vacuole marker), *white bar*; Ams1, *black bar*; α-glucosidase (cytosol marker), *light gray bar*; NADPH-cytochrome *c* reductase (ER marker), *dark gray bar*. Vacuoles were purified at least four times for each strain shown, and the total enzyme activity recovered in the vacuole fraction was divided by the total activity loaded on the gradient to obtain the percentage of recovery. Average recovery values are shown with error calculated as the standard deviation. *B*, mutants defective in both autophagy and the Cvt pathway are also defective in vacuolar delivery of Ams1. Ams1 is not recovered in the vacuole fractions from *apg1*, *apg7*, *apg9*Δ, *apg14*, and *aut7* strains. Percentage of recovery was as determined for *A*. The *cvt17* mutant accumulates Cvt vesicles within the vacuole, and shows equivalent vacuole recovery of Ams1 due to the accumulation of Ams1 within these vesicles.

for monitoring vacuolar delivery of Ams1.

We next examined whether Ams1 was delivered to the vacuole in strains defective specifically in the Cvt pathway. The *cvt3* and *cvt9* mutants accumulate the precursor form of API but are relatively normal for autophagy (11, 25). The Cvt9 protein interacts with the Apg1 kinase and may be part of a complex that includes Apg13, Apg17, and Vac8 (25–27). The *CVT3* gene has not been cloned, but the *cvt3* mutant appears to be defective in vesicle formation/completion because prAPI is protease-sensitive in this strain (16). The percent recovery of CPY-invertase was comparable in wild type and mutant strains, indicating that its delivery to the vacuole was not affected by *cvt* mutations (Fig. 2*A*). Accordingly, CPY-invertase is a useful marker for comparison to Ams1. Total Ams1 activity for wild type and mutant strains was comparable. However, the Ams1 activity in the vacuolar fraction of the *cvt3* and *cvt9* mutants was negligible, indicating that Cvt components are required for the transport of Ams1 to the vacuole (Fig. 2*A*). Contamination of the vacuolar fraction by other organelles or cytosol was determined by assaying the purified vacuole fraction for NAPDH-cytochrome *c* reductase activity (ER marker) and α-glucosidase (cytosol marker), respectively (Fig. 2*A*). The low level of Ams1 recovered in the purified vacuole fraction from most mutant strains was not substantially higher than the level of contamination from cytoplasmic markers. These data indicate Ams1 utilizes the Cvt pathway for vacuolar delivery under vegetative growth conditions.

We next examined mutants that are defective both in autophagy and the Cvt pathway. We decided to include in the analysis mutants that were blocked at different stages of the Cvt and autophagy (Apg) pathways (Table I). For example, the Apg1 kinase appears to be part of a complex that may be involved in regulating the conversion between the Cvt and Apg pathways (25, 27). Apg7 is a homolog of the E1 ubiquitin activating enzyme (28, 29). This protein is required for the conjugation of Apg12 to Apg5 and also for the addition of phosphatidylethanolamine to Aut7 (30, 31). The Aut7 protein is the only characterized component of these pathways that shows a substantial up-regulation of synthesis under autophagy-inducing conditions (32, 33). Aut7 is required for completion of Cvt vesicles and for expansion of the autophagosome membrane (34). Finally, Cvt17 is required for the breakdown of subvacuolar vesicles. The Cvt and autophagy pathways utilize double-membrane cytosolic vesicles to sequester cytoplasmic constituents. Fusion of these vesicles with the vacuole results in the release of a single-membrane subvacuolar vesicle, either a Cvt or autophagic body depending on the nutrient conditions. These subvacuolar vesicles are subsequently degraded within the vacuole lumen in a process that is dependent on Cvt17 and the vacuolar hydrolase proteinase B (35, 36).

The Ams1 activity recovered in vacuole fractions of most *apg*, *aut*, and *cvt* mutants was again negligible (Fig. 2*B*). As expected, the one exception was the *cvt17* mutant (Fig. 2*B*). The recovery of vacuolar Ams1 activity in *cvt17* was similar to that of CPY-invertase, indicating that Ams1 was located within vacuoles in the *cvt17* strain, presumably within Cvt bodies. Similar results were seen with a *pep4*Δ mutant strain that accumulates subvacuolar vesicles due to a defect in activation of proteinase B (data not shown). The dependence of Ams1 localization on Cvt, Apg, and Aut components suggests that Ams1 delivery to the vacuole requires both the Cvt and Apg components under vegetative conditions, and represents the second biosynthetic cargo protein that utilizes the Cvt pathway for vacuolar delivery.

Ams1 Is Imported as an Oligomer—Precursor API is oligomerized in the cytosol to form a dodecamer (7). The dodecameric form is maintained during the import process. The dodecameric precursor is ~732 kDa in mass and is too large to translocate through a proteinaceous channel such as the ER translocon. Accordingly, the particular biosynthesis of prAPI necessitates the use of a vesicle-mediated import mechanism such as the Cvt pathway. Because the *cvt* mutants lacked the ability to import Ams1, we were interested to see if oligomerization was a characteristic of this second cargo protein.

To determine whether oligomerization of Ams1 took place prior to import, wild type and mutant strains were analyzed by glycerol density gradients (Fig. 3). Protein extracts were prepared under native conditions and separated on a 20–50%

TABLE I
Characterized genes required for Ams1 targeting

Gene	Characteristics	References
Pathway induction and vesicle formation		
Kinase signaling system		
APG1	SER or THR protein kinase that interacts with Apg13, Apg17, and Cvt9	(25–27, 47)
APG9	Integral membrane protein	(15)
APG14	Peripheral membrane protein, interacts with Apg6 as part of Vps15/Vps34 kinase complex	(38, 48)
CVT9	Interacts with Apg1 kinase, specific for Cvt pathway	(25, 27)
CVT3	Required for vesicle formation/completion, specific for Cvt pathway	(10, 11, 16)
APG protein conjugation system		
APG7	E1 ubiquitin activating enzyme homolog, required for conjugation of Apg12 to Apg5, and for lipidation of Aut7	(28–31)
Size regulation of the autophagosome		
AUT7	Up-regulation by starvation, required for expansion of autophagosome	(31, 33, 34, 39)
Vesicle breakdown		
CVT17	Lipase homolog	(35)

glycerol density gradient in the presence of βOG detergent as described under "Experimental Procedures." As a control in this experiment, we analyzed the migration of API. The mature form of API peaked at fraction 7 of the gradient in agreement with our previous studies, indicating that it is present in the vacuole as a dodecamer (Fig. 3*A*; Ref. 7). Similarly, Ams1 from total cell lysates did not migrate on the gradient at a size expected for a monomer. Ams1 peaked at fraction 6, which corresponded to a molecular mass of 450–669 kDa based on marker protein analysis. The peptide antiserum to Ams1 cross-reacted with a diffuse background band (see Fig. 1*B*, *lane 5*) that migrated at fractions 3 and 4 of the glycerol gradient. To verify that Ams1 was not migrating at this part of the gradient, we examined the oligomeric state of the protein using anti-HA serum and a strain where the chromosomal *AMS1* locus had been replaced with an HA-tagged *AMS1* gene (see "Experimental Procedures"). Again, we found that Ams1 peaked at fraction 6 and no material was detected at the less dense region of the gradient (Fig. 3*A*). Therefore, in wild type cells, Ams1 appears to exist as an oligomer composed of 4–6 of the 122-kDa species.

We next wanted to determine if Ams1 was present as an oligomer in the cytosol and if so, whether it retained its oligomeric structure during import into the vacuole. Accordingly, we examined *apg* and *cvt* mutant strains to determine the oligomeric state prior to and following sequestration by Cvt vesicles. As noted above, the *apg7*/*cvt2* mutant is defective in the function of an E1-like protein (28, 29) and is required for both the Cvt and Apg pathways. The *apg7* mutant is blocked at the vesicle formation/completion step and accumulates prAPI in a membrane-bound form that is not within a completely enclosed vesicle. Ams1 peaked at fraction 6 of the glycerol gradient in the *apg7* mutant (Fig. 3*B*). Because this mutant is blocked in vacuolar delivery of Ams1 (Fig. 2*B*), these data suggest that Ams1 oligomerizes in the cytosol. As discussed above, the *cvt17* strain is defective in the breakdown of subvacuolar vesicles that result from the Cvt and Apg pathways. Ams1 was found to exist as an oligomer in the *cvt17* strain (Fig. 3*C*). The appearance of oligomeric Ams1 in the cytosol and in subvacuolar vesicles suggests that it maintains its oligomeric state during the import process.

Ams1 Arrives in the Vacuole by the Autophagy Pathway under Starvation Conditions—Precursor API is delivered to the vacuole by the Cvt or autophagy pathway depending on the nutrient conditions (9). To examine the localization of Ams1 under autophagic conditions, we followed the protein *in vivo* by confocal microscopy. Ams1 was placed under the control of a copper-inducible promoter and fused to YFP as described under "Experimental Procedures." Yeast cells were labeled with the dye FM 4–64 to mark the vacuole (23) and incubated under nitrogen starvation conditions (SD–N) for 12 h to induce autophagy and allow import of the hybrid protein. In SD–N, Ams1YFP was seen accumulating in the subvacuolar vesicles of *cvt17* and *pep4*Δ strains (Fig. 4) consistent with the vacuole fractionation data (Fig. 2*B*, data not shown). The *apg1* and *apg7* strains that are defective in autophagy showed no subvacuolar accumulation of Ams1YFP (Fig. 4), nor did strains that harbored a copper-inducible YFP construct alone (data not shown). Appearance of Ams1YFP in the vacuole was dependent on components of the autophagic pathway. These data demonstrate that Ams1 delivery to the vacuole was mediated by autophagosomes under conditions that induce autophagy.

DISCUSSION

Ams1 Is a Second Cargo Protein of the Cvt Pathway—Resident hydrolases of the vacuole/lysosome typically transit to the vacuole through a portion of the secretory pathway during biosynthesis. An alternate route, the Cvt pathway, is utilized by the vacuolar hydrolase API. The distinct characteristic of this biosynthetic route is the formation of double-membrane vesicles that sequester dodecameric prAPI in the cytosol. Under starvation conditions, this large oligomeric protein complex is taken to the vacuole via autophagy, which is morphologically and mechanistically similar to the Cvt pathway. Common gene products are involved in Cvt vesicle/autophagosome formation, vesicle fusion to the vacuole, and breakdown of vesicles delivered to the vacuole (for a detailed review, see Ref. 37). Many of these components act prior to vesicle formation such as Apg1, Apg7, Apg9, and Apg14 (15, 27, 28, 33, 38). Aut7 also acts at the stage of vesicle formation/completion but, unlike these other components, travels to the vacuole inside of the vesicles (31, 39). Finally, Cvt17 and Prb1 are critical for breakdown of the subvacuolar vesicles (35, 36). Opposing features of the selective Cvt pathway and non-selective autophagy occur at points of regulation, specificity, and cargo capacity. Some components required for delivery of proteins from the cytoplasm to the vacuole are specifically required for the Cvt pathway and others for autophagy. For example, selective vesicular targeting by the Cvt pathway depends on Cvt3, Cvt9, and Vac8 (9, 25, 26), whereas Apg17 is only needed for autophagy (27). Until now, prAPI was the only specific cargo protein that was definitively

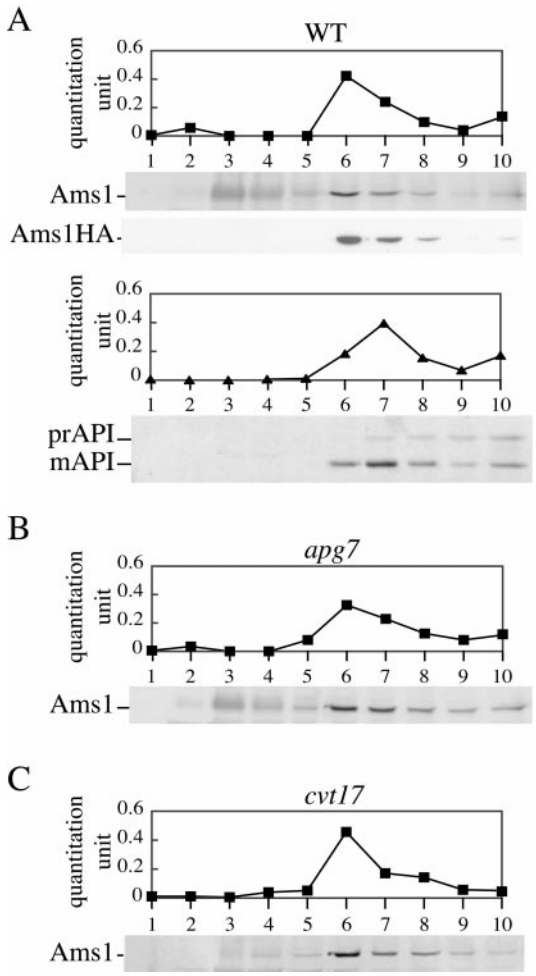

FIG. 3. **Ams1 transits to the vacuole as an oligomer.** *A*, wild type (*WT*) cells harboring the CEN Ams1 plasmid pCuAMS1(414) were grown to early log phase and induced with 50 μM copper sulfate for 1 h. Strain MHY11 (*AMS1*::*AMS1*-HA) was grown to early log phase and harvested directly. 20 A_{600} units of cells were lysed with glass beads, mixed with βOG detergent (2% final concentration), and loaded on a 20–50% glycerol gradient. Ten fractions of 200 μl were collected from the top and examined by immunoblot. Immunoblots were probed with anti-Ams1, anti-HA, or anti-API antisera and then quantitated using the Vistra detection reagents as described under "Experimental Procedures." Ams1 peaked as an oligomeric complex in fraction 6, whereas mAPI peaked at fraction 7 (7). Protein standards run on an identical gradient included: bovine serum albumin (66 kDa, fraction 3), aldolase (158 kDa, fraction 4), catalase (240 kDa, fraction 5), apoferritin (450 kDa, fraction 6), urease (545 kDa, fraction 6), and thyroglobulin (669 kDa, fraction 6). Note that the diffuse band in fractions 3 and 4 of the gradient detected with peptide antiserum is a cross-reacting contaminant and was not included in the quantification. *B* and *C*, oligomerization of Ams1 occurs in the cytosol and is maintained during vacuolar delivery. Native protein extracts from the *apg7* and *cvt17* mutant strains harboring pCuAMS1(414) were analyzed by glycerol gradients as in *A*. Ams1 is an oligomer in *apg7*, a mutant that is defective in vacuolar delivery of Ams1, and in *cvt17* that is defective in the breakdown of Cvt bodies.

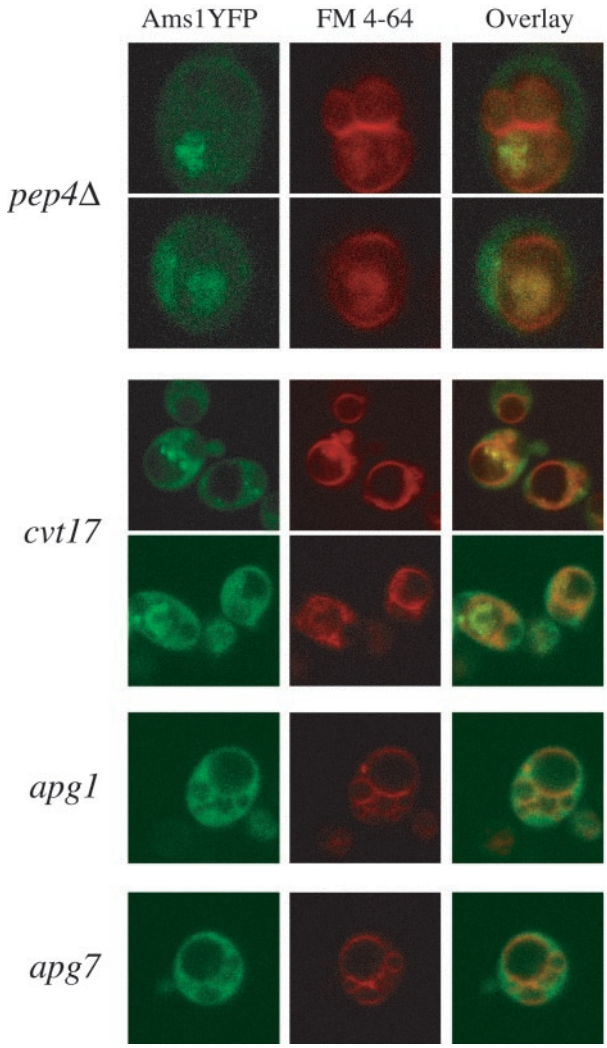

FIG. 4. **Ams1 is delivered to the vacuole by autophagy.** The Ams1YFP fusion protein was expressed in *cvt17*, *pep4*Δ, *apg1*, and *apg7* cells and visualized by confocal microscopy using the GFP channel as described under "Experimental Procedures." Vacuoles were labeled with FM 4–64, and cells were starved in SD−N for 12 h. Ams1YFP accumulates in subvacuolar vesicles of *cvt17* and *pep4*Δ strains under nitrogen starvation conditions. Ams1 is not delivered to the vacuole in *apg1* and *apg7* strains that show only cytosolic localization of Ams1YFP.

shown to use the Cvt pathway. In this study, we have identified a second cargo protein of the Cvt pathway, α-mannosidase.

Ams1 has been the canonical vacuole/lysosome membrane marker protein (40), but, until now, its mode of import in *Saccharomyces cerevisiae* was unclear. Like API, Ams1 is not glycosylated, nor does it utilize the secretory pathway (12). A decade has passed since researchers first attempted to define the import mechanism for Ams1. This is in part due to the difficulty of working with this protein. Ams1 is made at low levels during vegetative growth. In addition, prAPI undergoes proteolytic removal of its amino-terminal propeptide region coincident with vacuole import and enzyme activation. In contrast, a kinetically relevant processing event for Ams1 is not discernible, nor is the activation of Ams1 dependent on vacuole localization (12). Previously, import kinetics for Ams1 were assessed by its Pep4-dependent cleavage (12). In that study, cells were stressed by heat shock and then radiolabeled at 37 °C. Under these conditions, the half-time of delivery was determined to be ~10 h. However, the cleaved protein product was not localized subcellularly. This time frame also does not satisfy basal transport requirements of a cell that is growing with a 1.5-h doubling rate, as is the case in SMD . This Pep4-dependent cleavage event, therefore, does not appear to be a valid way to monitor vacuole delivery for Ams1. In fact, protease-susceptible sites present within Ams1 result in a 73-kDa polypeptide upon the addition of exogenous protease (12) or under environmental stress conditions (Fig. 1*B*). It is currently unclear whether there is a physiological significance to the proteolytic conversion of the 122-kDa Ams1 to the 73-and 31-kDa forms.

In contrast to previous studies, we conclude that Ams1 is not cleaved to a mature form directly upon delivery to the vacuole.

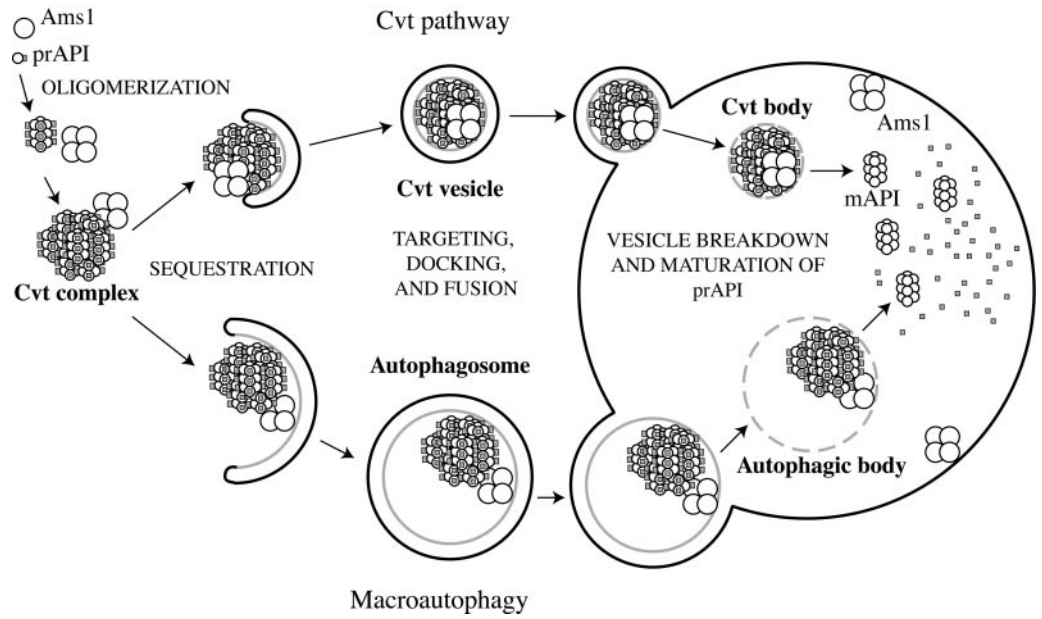

FIG. 5. **Model for Ams1 delivery to the vacuole.** Like prAPI, Ams1 assembles into an oligomer in the cytosol and is sequestered by membrane that forms either a Cvt vesicle (nutrient-rich conditions) or an autophagosome (starvation conditions). It is not known whether Ams1 associates with the prAPI-containing Cvt complex. The completed vesicle targets to and fuses with the vacuole, releasing the Cvt body or autophagic body into the vacuole lumen. Subsequent vesicle breakdown releases the cargo. Unlike prAPI, proteolytic maturation of Ams1 does not occur concomitant with vacuolar import. Oligomeric Ams1 becomes peripherally associated with the vacuole membrane.

Because proteolytic processing does not appear to occur coincident with vacuolar delivery, it is problematic to determine the kinetics of import for Ams1. We speculate that the half-time for delivery of Ams1 is similar to that of prAPI (20–30 min; Ref. 11) because of the dependence on the selective vacuolar targeting gene products such as Cvt3 and Cvt9 (Fig. 2*A*). Due to the absence of a convenient gel mobility assay to follow localization, we relied on subcellular fractionation to monitor vacuolar Ams1 delivery. All *cvt*, *apg*, and *aut* mutants examined, with the exception of *cvt17*, were found to be defective in vacuolar delivery of Ams1 (Fig. 2). The recovery of Ams1 in the vacuoles of the *cvt17* strain under vegetative conditions is consistent with the premise that Ams1 is a Cvt cargo protein. Subvacuolar vesicles containing prAPI have been shown to accumulate in the *cvt17* mutant as well as in a *pep4*Δ strain (9, 11).

Recently, we have characterized the Cvt19 protein as a receptor for resident vacuolar hydrolases that utilize the Cvt pathway.[2] Targeting of prAPI under starvation conditions requires Cvt19 even though nonspecific autophagy is functional in the *cvt19*Δ strain. The *cvt19*Δ mutant is defective in vacuolar localization of Ams1.[2] Hence, Cvt19 is required for the specific transport of both cargo proteins through the Cvt pathway and at least for prAPI by autophagy and may represent a limiting factor for import of these resident hydrolases. These data support the conclusion that Ams1 utilizes the Cvt pathway.

Ams1 Is Imported into the Vacuole as an Oligomer—Gel filtration chromatography has shown that vacuolar Ams1 is a 560-kDa hetero-oligomer (24). Although a 107-kDa form was only reported from *pep4*Δ cells (12), we observed a form migrating at 122 kDa in wild type cells (Fig. 1). The 122-kDa mass is in closer agreement to the predicted size of Ams1 based on its deduced amino acid sequence. In the present study, we show that the 122-kDa form of Ams1 assembled into an oligomeric conformation in the cytosol (Fig. 3*B*). Furthermore, this state was maintained throughout vacuolar delivery (Fig. 3*C*). It is apparent from the data presented here that vacuolar Ams1 is most likely a homo-oligomer composed of 122-kDa subunits. These results suggest that one interesting feature of the Cvt pathway is that the cargo proteins, prAPI and Ams1, are imported as oligomers (Ref. 7; Fig. 3*C*).

Crossing a membrane as an intact oligomeric complex is a major challenge. Dodecameric prAPI is ~732 kDa in mass, too large to translocate through a proteinaceous channel such as that present in the ER. Accordingly, prAPI is sequestered within vesicles during their formation in the cytosol. Similarly, Ams1 uses this pathway for vacuolar localization. There are two ways to interpret the oligomeric assembly data. Precursor API appears to be unstable as a monomer.[3] Vacuolar proteins that need to exist as oligomers either for stability or function may need to utilize the Cvt pathway for localization. Conversely, it is possible that these proteins form oligomers so that they are imported more efficiently by the Cvt pathway and autophagy to satisfy other cellular demands. For example, both Ams1 and API are up-regulated during starvation. Macromolecular turnover is essential under these conditions. By coupling autophagy with the import of certain key hydrolases, the cell ensures the presence of both substrates and degradative enzymes within the vacuole. There is an apparent redundancy of hydrolases within the vacuole including carboxypeptidases S and Y, aminopeptidases I and Y, and proteinases A and B. The Cvt pathway presents an alternative mechanism for delivering hydrolases to the vacuole, ensuring the presence of at least minimal degradative capacity if the Vps route to the vacuole is defective. There are additional reasons for Ams1 to utilize the Cvt pathway. Ams1 is membrane-associated but is not an integral membrane protein. It lacks a signal sequence or hydrophobic domain that could act as an internal uncleaved signal sequence so that it is unable to enter the secretory pathway. Finally, Ams1 is a mannose glycosidase that appears to be constitutively active. It would be problematic for this enzyme to traverse the secretory pathway along with mannosylated glycoproteins.

[2] Scott, S. V., Guan, M. U., Kim, J., and Klionsky, D. J. (2001) *Molec. Cell*, in press.

[3] Andrei-Selmer, C., Knüppel, A., Satyanarayana, C., Heese, C., and Schu, P. V. (2001) *J. Biol. Chem.* **276,** 11606–11614.

Ams1 Utilizes the Autophagy Pathway for Vacuolar Delivery under Starvation Conditions—Environmental stress conditions such as starvation signal a major change in yeast physiology. Although the Cvt pathway exists primarily as a biosynthetic route to the vacuole, autophagy is capable of delivering both resident vacuolar hydrolases and bulk quantities of their substrates to this organelle. It is therefore reasonable to expect autophagy to carry Ams1 into the vacuole during nutrient limitation. We investigated the localization of an Ams1YFP fusion protein under starvation conditions. Both *cvt17* and *pep4*Δ mutant strains are defective in breakdown of subvacuolar vesicles, independent of their origin (9, 35). In addition to localizing Ams1 activity to the vacuole fraction under vegetative conditions (Fig. 2*B* and data not shown), both strains show an abundance of the Ams1YFP fusion protein within accumulated subvacuolar vesicles in cells starved for nitrogen (Fig. 4). Therefore, like prAPI, Ams1 also utilizes autophagy to reach the vacuole. Based on these data, we propose a model for Ams1 import shown in Fig. 5.

The importance of understanding the molecular mechanisms of protein transport in the lower eukaryotes is becoming more evident as human genome data become available. Although it has not yet been characterized, the human homologue to *AMS1* was recently isolated from cDNA (GenBank accession no. AF044414). The highly homologous encoded protein (35% identical, 51% similar to Ams1 according to BLAST results; Ref. 41) is more closely related to the isolated rat α-mannosidase than the yeast enzyme, as expected. Extensive sequence comparison between the known α-mannosidases (EC 3.2.1.24) in fungi with a rat homologue has been described (42). None of these protein family members have any classical signal sequence or membrane-spanning domains, suggesting that they may not transit through the secretory pathway. Analysis of the known Ams1 homolog from rat suggested that it is localized to the ER and the cytosol (43, 44); however, to our knowledge, the possibility of a lysosomal localization for this protein has not been fully explored. Ams1 and its homologs were recently categorized as the most ancestral α-mannosidase family in a global comparison within the α-mannosidase superfamily (45). Once the Ams1-like human homolog has been identified, it will be interesting to observe its intracellular localization and cell type/developmental expression pattern and determine whether a Cvt-like cytoplasm to lysosome pathway exists in addition to the established autophagy pathway in humans (46). Perhaps the ancestral targeting pathway has been maintained for this putative protein. Continued study of the cytoplasm to vacuole targeting pathway in yeast and a search for additional Cvt cargo will broaden our understanding of vacuole/lysosome biogenesis.

Acknowledgments—We thank Drs. John Kim, Sidney Scott, and Sarah Teter for critically reading the manuscript; Dr. Tanya Harding for constructing the *ams1*Δ strain; and Drs. Neta Dean, Dennis Thiele, Michael Kuranda, and Phillips Robbins for their generous gift of plasmids.

REFERENCES

1. Keegstra, K., and Froehlich, J. E. (1999) *Curr. Opin. Plant Biol.* **2,** 471–476
2. Rassow, J., and Pfanner, N. (2000) *Traffic* **1,** 457–464
3. Subramani, S., Koller, A., and Snyder, W. B. (2000) *Annu. Rev. Biochem.* **69,** 399–418
4. Teter, S. A., and Klionsky, D. J. (1999) *Trends Cell Biol.* **9,** 428–431
5. McNew, J. A., and Goodman, J. M. (1994) *J. Cell Biol.* **127,** 1245–1257
6. Klionsky, D. J., Cueva, R., and Yaver, D. S. (1992) *J. Cell Biol.* **119,** 287–299
7. Kim, J., Scott, S. V., Oda, M. N., and Klionsky, D. J. (1997) *J. Cell Biol.* **137,** 609–618
8. Scott, S. V., Baba, M., Ohsumi, Y., and Klionsky, D. K. (1997) *J. Cell Biol.* **138,** 37–44
9. Baba, M., Osumi, M., Scott, S. V., Klionsky, D. J., and Ohsumi, Y. (1997) *J. Cell Biol.* **139,** 1687–1695
10. Harding, T. M., Hefner-Gravink, A., Thumm, M., and Klionsky, D. J. (1996) *J. Biol. Chem.* **271,** 17621–17624
11. Scott, S. V., Hefner-Gravink, A., Morano, K. A., Noda, T., Ohsumi, Y., and Klionsky, D. J. (1996) *Proc. Natl. Acad. Sci. U. S. A.* **93,** 12304–12308
12. Yoshihisa, T., and Anraku, Y. (1990) *J. Biol. Chem.* **265,** 22418–22425
13. Kuranda, M. J., and Robbins, P. W. (1987) *Proc. Natl. Acad. Sci. U. S. A.* **84,** 2585–2589
14. Robinson, J. S., Klionsky, D. J., Banta, L. M., and Emr, S. D. (1988) *Mol. Cell. Biol.* **8,** 4936–4948
15. Noda, T., Kim, J., Huang, W.-P., Baba, M., Tokunaga, C., Ohsumi, Y., and Klionsky, D. J. (2000) *J. Cell Biol.* **148,** 465–479
16. Harding, T. M., Morano, K. A., Scott, S. V., and Klionsky, D. J. (1995) *J. Cell Biol.* **131,** 591–602
17. Hutchins, M. U., Veenhuis, M., and Klionsky, D. J. (1999) *J. Cell Sci.* **112,** 4079–4087
18. Labbé, S., Zhu, Z., and Thiele, D. J. (1997) *J. Biol. Chem.* **272,** 15951–15958
19. Sikorski, R. S., and Hieter, P. (1989) *Genetics* **122,** 19–27
20. Johnson, L. M., Bankaitis, V. A., and Emr, S. D. (1987) *Cell* **48,** 875–885
21. Haas, A. (1995) *Methods Cell Sci.* **17,** 283–294
22. Opheim, D. J. (1978) *Biochim. Biophys. Acta* **524,** 121–130
23. Vida, T. A., and Emr, S. D. (1995) *J. Cell Biol.* **128,** 779–792
24. Yoshihisa, T., Ohsumi, Y., and Anraku, Y. (1988) *J. Biol. Chem.* **263,** 5158–5163
25. Kim, J., Kamada, Y., Stromhaug, P. E., Guan, J., Hefner-Gravink, A., Baba, M., Scott, S. V., Ohsumi, Y., Dunn, W. A., Jr., and Klionsky, D. J. (2001) *J. Cell Biol.* **153,** 381–396
26. Scott, S. V., Nice, D. C., III, Nau, J. J., Weisman, L. S., Kamada, Y., Keizer-Gunnink, I., Funakoshi, T., Veenhuis, M., Ohsumi, Y., and Klionsky, D. J. (2000) *J. Biol. Chem.* **275,** 25840–25849
27. Kamada, Y., Funakoshi, T., Shintani, T., Nagano, K., Ohsumi, M., and Ohsumi, Y. (2000) *J. Cell Biol.* **150,** 1507–1513
28. Kim, J., Dalton, V. M., Eggerton, K. P., Scott, S. V., and Klionsky, D. J. (1999) *Mol. Biol. Cell* **10,** 1337–1351
29. Tanida, I., Mizushima, N., Kiyooka, M., Ohsumi, M., Ueno, T., Ohsumi, Y., and Kominami, E. (1999) *Mol. Biol. Cell* **10,** 1367–1379
30. Mizushima, N., Noda, T., Yoshimori, T., Tanaka, Y., Ishii, T., George, M. D., Klionsky, D. J., Ohsumi, M., and Oshumi, Y. (1998) *Nature* **395,** 395–398
31. Ichimura, Y., Kirisako, T., Takao, T., Satomi, Y., Shimonishi, Y., Ishihara, N., Mizushima, N., Tanida, I., Kominami, E., Ohsumi, M., Noda, T., and Ohsumi, Y. (2000) *Nature* **408,** 488–492
32. Kirisako, T., Ichimura, Y., Okada, H., Kabeya, Y., Mizushima, N., Yoshimori, T., Ohsumi, M., Takao, T., Noda, T., and Ohsumi, Y. (2000) *J. Cell Biol.* **151,** 263–275
33. Huang, W.-P., Scott, S. V., Kim, J., and Klionsky, D. J. (2000) *J. Biol. Chem.* **275,** 5845–5851
34. Abeliovich, H., Dunn, W. A., Jr., Kim, J., and Klionsky, D. J. (2000) *J. Cell Biol.* **151,** 1025–1034
35. Teter, S. A., Eggerton, K. P., Scott, S. V., Kim, J., Fischer, A. M., and Klionsky, D. J. (2001) *J. Biol. Chem.* **276,** 2083–2087
36. Takeshige, K., Baba, M., Tsuboi, S., Noda, T., and Ohsumi, Y. (1992) *J. Cell Biol.* **119,** 301–311
37. Kim, J., and Klionsky, D. J. (2000) *Annu. Rev. Biochem.* **69,** 303–342
38. Kihara, A., Noda, T., Ishihara, N., and Ohsumi, Y. (2001) *J. Cell Biol.* **152,** 519–530
39. Kim, J., Huang, W.-P., and Klionsky, D. J. (2001) *J. Cell Biol.* **152,** 51–64
40. van der Wilden, W., Matile, P., Schellenberg, M., Meyer, J., and Wiemken, A. (1973) *Z. Naturforsch.* **28c,** 416–421
41. Tatusova, T. A., and Madden, T. L. (1999) *FEMS Microbiol. Lett.* **174,** 247–250
42. Eades, C. J., Gilbert, A.-M., Goodman, C. D., and Hintz, W. E. (1998) *Glycobiology* **8,** 17–33
43. Bischoff, J., Moremen, K., and Lodish, H. F. (1990) *J. Biol. Chem.* **265,** 17110–17117
44. Grard, T., Herman, V., Saint-Pol, A., Kmiecik, D., Labiau, O., Mir, A.-M., Alonso, C., Verbert, A., Cacan, R., and Michalski, J.-C. (1996) *Biochem. J.* **316,** 787–792
45. Gonzalez, D. S., and Jordan, I. K. (2000) *Mol. Biol. Evol.* **17,** 292–300
46. Mizushima, N., Sugita, H., Yoshimori, T., and Ohsumi, Y. (1998) *J. Biol. Chem.* **273,** 33889–33892
47. Matsuura, A., Tsukada, M., Wada, Y., and Ohsumi, Y. (1997) *Gene* (*Amst.*) **192,** 245–250
48. Kametaka, S., Okano, T., Ohsumi, M., and Ohsumi, Y. (1998) *J. Biol. Chem.* **273,** 22284–22291